

Tricyanoborane-Functionalized Anionic N-Heterocyclic Carbenes: Adjustment of Charge and Stereo-Electronic Properties

Ludwig Zapf,^[a] Sven Peters,^[a] Rüdiger Bertermann,^[a] Udo Radius,^{*,[a]} and Maik Finze^{*,[a]}

Dedicated to Professor Helge Willner on the occasion of his 75th birthday

Abstract: The 1-methyl-3-(tricyanoborane)imidazolin-2-ylidene anion (**2**) was obtained in high yield by deprotonation of the B(CN)₃-methylimidazole adduct **1**. Regarding charge and stereo-electronic properties, anion **2** closes the gap between well-known neutral NHCs and the ditopic dianionic NHC, the 1,3-bis(tricyanoborane)imidazolin-2-ylidene dianion (**IIb**). The influence of the number of N-bonded tricyanoborane moieties on the σ -donating and π -accepting properties of NHCs was assessed by quantum chemical calculations and verified by experimental data on **2**, **IIb**, and 1,3-dimeth-

ylimidazolin-2-ylidene (**IME**, **IIa**). Therefore NHC **2**, which acts as a ditopic ligand via the carbene center and the cyano groups, was reacted with alkyl iodides, selenium, and [Ni(CO)₄] yielding alkylated imidazoles **3** and **4**, the anionic selenium adduct **5**, and the anionic nickel tricarbonyl complex **8**, respectively. The results of this study prove that charge, number of coordination sites, buried volume (%V_{bur}) and σ -donor and π -acceptor abilities of NHCs can be effectively fine-tuned via the number of tricyanoborane substituents.

Introduction

N-heterocyclic carbenes (NHCs) are an important class of compounds with widespread applications in chemical industry and academia, for example in organo- and transition metal catalysis or in medical applications.^[1] The properties of NHCs, namely their strong σ -donor and π -acceptor ability, can be tuned over a wide range. Especially, the introduction of substituents at the central NHC ring is of importance for the variation of the nature of the carbene. Since the isolation of the first stable, crystalline NHC by Arduengo and coworkers (**A**, Figure 1) in the early 90ies of the last century,^[2] a wealth of different NHCs has been synthesized and their physicochemical and chemical properties have been explored, in detail.

The introduction of borane substituents at the NHC core is a straightforward and promising strategy towards anionic NHCs with tunable electronic and steric properties.^[3] Triscarbene **B**

[a] L. Zapf, S. Peters, Dr. R. Bertermann, Prof. Dr. U. Radius, Prof. Dr. M. Finze
Institute for Sustainable Chemistry & Catalysis with Boron (ICB)
Institute of Inorganic Chemistry
Julius-Maximilians-Universität Würzburg,
Am Hubland, 97074 Würzburg (Germany)
E-mail: u.radius@uni-wuerzburg.de
maik.finze@uni-wuerzburg.de
Homepage: <http://go.uni.wue.de/finze-group>
<http://www.ak-radius.de>

Supporting information for this article is available on the WWW under <https://doi.org/10.1002/chem.202200275>

© 2022 The Authors. Chemistry - A European Journal published by Wiley-VCH GmbH. This is an open access article under the terms of the Creative Commons Attribution Non-Commercial NoDerivs License, which permits use and distribution in any medium, provided the original work is properly cited, the use is non-commercial and no modifications or adaptations are made.

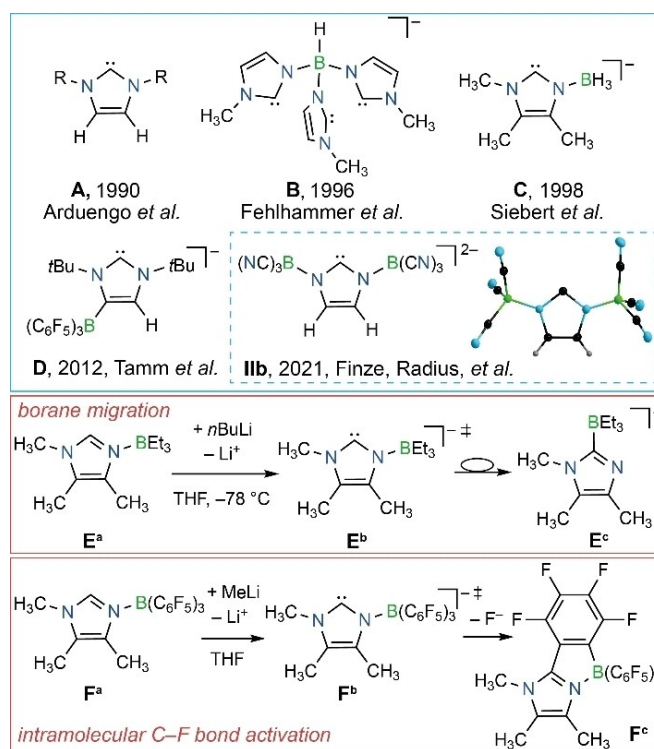


Figure 1. Neutral Arduengo-type NHCs (**A**), selected anionic borane-substituted NHCs (**B–D**), the dianionic bis(borane)-substituted NHC **IIb**, and intramolecular follow-up reactions of in situ generated carbenes **E^b** and **F^b**.

(Figure 1)^[4] was the first representative of this class of compounds and since then related anionic tris- and biscarbenes

have been described.^[5] Surprisingly, related NHCs with a non-bridging borane moiety at either one or both nitrogen atoms remain scarce. The BH₃-substituted N-heterocyclic carbene **C** (Figure 1) was the first example that was reported in 1998.^[6] Carbene **C** and related anionic NHCs with a single BH₃ group were used as ligands in transition metal coordination chemistry, in nucleophilic substitution reactions with tetrahalides, and in reactions with boranes.^[7] Another rare example of an anionic borane-substituted NHC with an alternative binding mode was described in 2012 (**D**, Figure 1).^[8]

Unlike **C**, the weakly coordinating borane moiety B(C₆F₅)₃ of imidazolin-2-ylidene **D** is not bonded to nitrogen but to the carbon backbone. The anionic borane substituted NHC **D** is not only a useful building block for the synthesis of unusual group 13, 16, and 17 derivatives,^[9] but also a versatile tool for the activation of organic compounds, and for the preparation of catalytically active transition metal complexes.^[8,9c,10]

In contrast to the formation of **C** and **D**, attempted synthesis of other borane-imidazole derivatives did not lead to the respective anionic carbene. For instance, deprotonation of 3-triethylborane-1,4,5-trimethylimidazole (**E**^a, Figure 1) resulted in **E**^c with a C_{carbene}–B bond, which was rationalized by an instant migration of the Et₃B group.^[7] Another example is the deprotonation of 3-tris(pentafluorophenyl)borane-1-methylimidazole (**F**^a, Figure 1) that gave the cyclisation product **F**^c, which was the result of an intramolecular nucleophilic attack of the carbene C atom at one of the C₆F₅ rings.^[11]

Recently, we reported on the synthesis of a new type of a borane-substituted NHC, the dianionic ditopic 1,3-bis(tricyanoborane)imidazolin-2-ylidene **IIb** (Figure 1).^[12] The reason for the unprecedented stability of dianion **IIb** are the B(CN)₃ moieties that are connected via B–N bonds to the central NHC core. Tricyanoborane is a Lewis superacid,^[13] which explains the very robust B–N bonds and thus the stability of **IIb**. The B(CN)₃ group results in very stable borate anions, in general.^[14] This includes tricyanoborates of the type [RB(CN)₃][–] (R=H,^[15] F,^[16] Cl,^[17] NC,^[16a,18] CH₃O,^[19] perfluoroalkyl,^[20] (fluoro)aryl^[21]), the hexacyanoborate dianion [B₂(CN)₆]^{2–},^[22] and the boron-centered nucleophile B(CN)₃^{2–}.^[23] Dianion **IIb** can coordinate to a metal center via the carbene C atom and the cyano groups of the B(CN)₃ units. The carbene center is shielded as evident from the buried volume (%V_{bur}) of 39.9%. Further experimental results of our preliminary study on **IIb** provided evidence for an increased σ-donor and π-acceptor ability compared to other unsaturated NHCs. To gain a more sophisticated insight into the influence of the B(CN)₃ group on the properties of NHCs, a comparison of the related NHCs 1,3-dimethylimidazolin-2-ylidene (**IMe**, **IIa**),^[24] 1-methyl-3-(tricyanoborane)imidazolin-2-ylidene (**2**), and **IIb** is necessary. Herein, we report on the synthesis of **2**, selected derivatives of **2**, **IIa**, and **IIb**, and a comparative experimental and theoretical study on the properties of the three related NHCs.

Results and Discussion

1-Methyl-3-(tricyanoborane)imidazole (**1**) was prepared from tricyanoborane-pyridine adduct (B(CN)₃py; py = pyridine)^[25] and 1-methylimidazole in acetonitrile (Figure 2). Since the starting materials are easily accessible and because of the high yield of more than 95%, **1** can be synthesized on a multigram scale. Neutral **1** melts at 182 °C and decomposes at 360 °C (DSC, onset). It is stable towards air, moisture, and water. It was characterized by NMR and vibrational spectroscopy, single-crystal X-ray diffraction (SC-XRD), and high-resolution mass spectrometry (HRMS). Single crystals of **1** were obtained by slow evaporation of an acetone solution (Figure 2). The B1–N3 distance of 155.3(2) pm is in the range of related B(CN)₃ Lewis base adducts, for example 157.1 pm in B(CN)₃py^[25a] or 153.4(4)/155.8(4) pm in lithium 1,3-bis(tricyanoborane)imidazolate.^[12]

With the neutral imidazole **1** as starting material in hand, its deprotonation was investigated. Lithium and potassium hexamethyldisilazide were found to be suitable bases for the formation of the 1-methyl-3-(tricyanoborane)imidazolin-2-ylidene anion **2**. Treatment of **1** with a small excess of LiHMDS in THF resulted in Li₂·THF_{0.5} as a solid in a yield of 85% (Figure 3). K₂·Et₂O_{0.5} precipitated upon addition of diethyl ether from the reaction mixture in THF and it was isolated in 96% yield (Figure 3). The selective deprotonation of **1** at the C2 atom to result in **2** was confirmed by NMR spectroscopy (Figure 3). The ¹¹B NMR signal is shifted from –25.5 (**1**) to –24.1 ppm (**2**). The signal of the backbone H atom at C5 (H5) of **2** reveals coupling to boron (⁴J(¹¹B,¹H)) that is not observed for **1** (Figure 3). The most significant difference was observed in the ¹³C{¹H} NMR spectrum for the C2 nucleus. Its signal was shifted from 139.7 (**1**) to 205.4 ppm (Li₂) or 211.9 ppm (K₂), which is in the typical range observed for C_{carbene} nuclei, for example 205.9 ppm for **IIb**,^[12] 215.2 ppm for **IIa**,^[24] or 211.2 ppm for **D**.^[8] Furthermore the signal is split into a quartet due to the coupling to ¹¹B with ²J(¹³C,¹¹B) of 11.8 Hz. This coupling constant is close to the coupling of the two ¹¹B nuclei with the C2

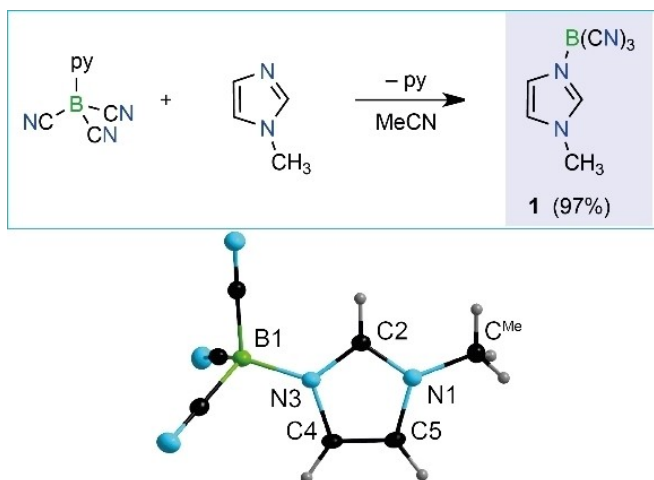


Figure 2. Synthesis and crystal structure of **1** (ellipsoids are drawn with 50% probability except for H atoms that are depicted with arbitrary radii).

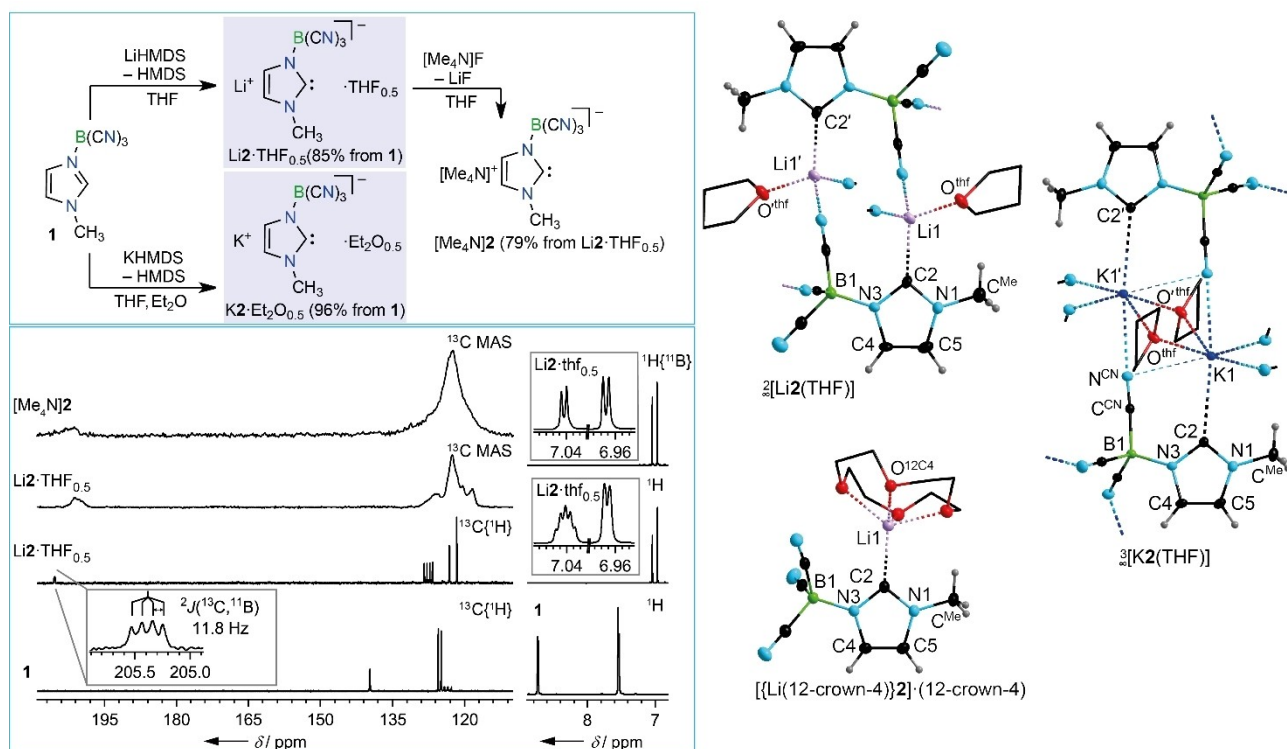


Figure 3. Syntheses of $\text{Li}^+\text{·THF}_{0.5}$, $\text{K}^+\text{·Et}_2\text{O}_{0.5}$, and $[\text{Me}_4\text{N}]^+\text{2}$ (top left), NMR spectra of 1, $\text{Li}^+\text{·THF}_{0.5}$ and $[\text{Me}_4\text{N}]^+\text{2}$ (bottom left). A dimer of $[\text{Li}^+\text{·THF}]$ and a unit of $[\{\text{Li}(\text{12-crown-4})\}_2\text{·(12-crown-4)}]$ in the crystal structures (right; ellipsoids are drawn with 50% probability except for H atoms that are depicted with arbitrary radii, disorder and H atoms of the THF solvate molecules and of the coordinated 12-crown-4 moiety are not shown and their C atoms are depicted as wireframe model, the co-crystallized 12-crown-4 molecule is omitted for clarity).

nucleus of **IIb** ($^2J(^{13}\text{C}, ^{11}\text{B}) = 11.7$ Hz).^[12] To evaluate if solvated anion **2** can be considered as NHC and not only as a lithio- or potassio-carbenoid, metathesis with $[\text{Me}_4\text{N}]^+\text{F}^-$ to yield $[\text{Me}_4\text{N}]^+\text{2}$ in a yield of 79% was performed (Figure 3). $[\text{Me}_4\text{N}]^+\text{2}$ was characterized by NMR and vibrational spectroscopy as well as by elemental analysis. The tetramethylammonium salt is stable and storable as a solid. In solution, anion **2** is methylated at the C2 atom by $[\text{Me}_4\text{N}]^+$ under formation of trimethylamine. Due to the relatively fast decomposition, we were not able to obtain a meaningful $^{13}\text{C}\{^1\text{H}\}$ NMR spectrum in solution. However, solid state ^{13}C MAS NMR spectra of both salts, $[\text{Me}_4\text{N}]^+\text{2}$ and $\text{Li}^+\text{·THF}_{0.5}$, respectively, were recorded (Figure 3). Surprisingly, a minor shift of the signal of the C2 nucleus from 200.7 (Li2) to 202.0 ppm ($[\text{Me}_4\text{N}]^+\text{2}$) was observed, supporting the assumption that the electronic influence of the Li^+ or K^+ cation on the anionic NHC **2** is small. This is in accordance with $\delta(^{13}\text{C})$ of **D** with Li^+ ($\delta(\text{C}2) = 217.4$ ppm) and $[\text{PPh}_4]^+$ ($\delta(\text{C}2) = 218.8$ ppm) as counter cation. In contrast to $[\text{Me}_4\text{N}]^+\text{2}$, $\text{Li}^+\text{·THF}_{0.5}$ and $\text{K}^+\text{·Et}_2\text{O}_{0.5}$ are thermally less robust than $\text{Li}^+\text{·THF}$ ($T_{\text{dec}} > 150^\circ\text{C}$)^[12] but more stable than **IIa**, which gradually decomposes already at room temperature.^[24] This trend in thermal stability highlights the stabilizing effect of the tricyanoborane moieties as substituent at the N atoms of NHCs.

Single crystals of $[\text{Li}^+\text{·THF}]$ were obtained from THF. The carbene units form cyclic dimers via bridging Li1 atoms (Figure 3). These dimers are interconnected to strands. The lithium ion is coordinated to the C2 carbene atom and to two CN groups of different anions **2**, which highlights the ditopic nature of **2**. The distorted tetrahedral coordination at the lithium cation is completed by a THF ligand. The Li–C2 distance of 217.0(6) pm is similar to related Li–C_{carbene} separations, for example 215.1(6) pm in $[\text{Li}^+\text{·IIb}(\text{THF})]$,^[12] 215.5(4) pm in $[(t\text{Bu}_2\text{Im})\text{Li}(\eta^5\text{-1,2,4-(Me}_3\text{Si)}_3\text{C}_5\text{H}_2)]$,^[26] and 209.2(2)/209.4(3) pm in $[\text{Li}^+\text{·THF}]_2$.^[8] Crystallization of $\text{Li}^+\text{·THF}_{0.5}$ from THF in the presence of 12-crown-4 led to single crystals of $[\{\text{Li}(\text{12-crown-4})\}_2\text{·(12-crown-4)}]$ (Figure 3). The Li ion in $[\{\text{Li}(\text{12-crown-4})\}_2\text{·(12-crown-4)}]$ is coordinated to the C2 carbene atom and to all four oxygen atoms of 12-crown-4. In contrast to $[\text{Li}^+\text{·THF}]$, the cyano N atoms do not participate in the coordination to lithium.

Single crystals of $[\text{K}^+\text{·THF}]$ were obtained by diffusion of hexane into THF. Two formula units of $\text{K}^+\text{·THF}$ form dimers, similar to $[\text{Li}^+\text{·THF}]$. The potassium cation adopts a distorted pentagonal bipyramidal coordination sphere spanned by one C_{carbene} atom, four CN groups, and two THF molecules (Figure 3).

The K1–C2 distance of 298.7(1) pm is similar to related K–C_{carbene} separations, for example 298.6(2) pm in $[\{\text{H}_2\text{C}(\text{iPr})_2\}\text{KN}(\text{SiMe}_3)_2]$.^[27] Compared to **1**, the B–N distance in **2** is slightly shorter (153.4(4) pm), whereas $d(\text{C}2\text{--N})$ are a little longer. Both differences reflect the increased electron density at the C2

carbene atom in **2**, which results in a slight weakening of the C2–N bonds, an increased basicity of the N atoms in the ring, and in turn stronger B–N bonds, similar to **IIb**.^[12]

DFT calculations (def2-TZVPP/B3LYP/D3(BJ)/COSMO [$\epsilon = \infty$]), for details see the Supporting Information) were performed to evaluate the electronic features of **2** in comparison to the neutral NHC **IIa**^[28] and the dianionic NHC **IIb**. For **IIa**, the electronic structure can be considered as a 6 π -electron aromatic system that is superimposed with the NHC carbene σ -type orbital, which is basically a sp_2 -type hybrid orbital. The latter is the HOMO of the molecule and lies at -6.36 eV calculated at this level of theory (see Figure 4). The carbene π -orbital of **IIa** is the LUMO + 1 (the LUMO is another orbital of the NHC π -system), mainly centered at the carbene C atom, and is mostly composed of the carbene p_x orbital. This unoccupied orbital lies at $+0.70$ eV, which leads to a σ/π -separation of 7.06 eV. This separation decreases continuously upon successive formal replacement of the methyl against $B(CN)_3^-$ substituents to 6.82 eV for **2** and 6.61 eV for **IIb**. The HOMO is always the NHC σ -orbital, whereas the relevant NHC π -orbital varies. In case of **IIa** it is the LUMO + 1, in case of **2** the LUMO + 3, and for **IIb** the LUMO + 6 (Figure 4). For the cyanoboron-substituted compounds, some $C\equiv N$ antibonding combinations are located in between the NHC σ - and π -orbitals. However, as $B(CN)_3$ substitution proceeds the NHC π -orbitals decrease in energy going from $+0.70$ eV (**IIa**) to $+0.58$ eV (**2**) to $+0.48$ eV (**IIb**), whereas the orbital energy of the HOMO increases going from -6.36 eV (**IIa**) to -6.24 eV (**2**) to -6.13 eV (**IIb**). Thus, the donor and the acceptor capabilities of the different NHCs increase in the row **IIa** < **2** < **IIb**, as was verified experimentally (see below).

To get a first impression on the basic reactivity of the anionic NHC **2** and to assess its σ -donating and π -accepting properties experimentally, **Li2** was reacted with methyl iodide,

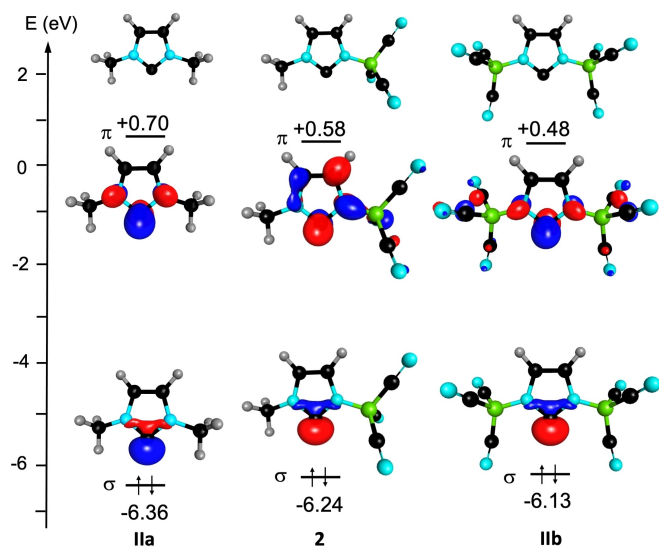


Figure 4. NHC σ - and π -orbitals of **IIa**, **2**, and **IIb**. Energies were calculated at the DFT/def2-TZVPP/B3LYP/D3(BJ)/COSMO [$\epsilon = \infty$] level of theory and orbital plots are drawn at the 0.1 isosurface.

the chalcogens sulfur, selenium, and tellurium, as well as nickel tetracarbonyl as archetypical reactions for organic, main-group, and transition-metal substrates. Methylation of **2** with methyl iodide afforded 1,2-dimethyl-3-(tricyanoborane)imidazole (**3**) in an internal yield of 52%. 1-Methyl-3-(tricyanoborane)imidazole (**1**) and the related ethylated imidazole **4** were obtained as side products in equimolar amounts (24%, Figure 5). Formation of **4** and **1** can be rationalized by a methylene intermediate, which is formed by deprotonation of **3** with unreacted **2**. The methylene intermediate subsequently reacts with methyl iodide to form **4** (Figure 5). The ethyl derivative **4** was obtained as sole product by the reaction of **2** and ethyl iodide. The synthesis of the related methylene derivate 1,3-dimethyl-2-methyleneimidazole was also accomplished by deprotonation of 1,2,3-trimethylimidazole with strong bases such as KHMDS or KH as reported previously.^[29] Anyway, considering all side products the reaction of **Li2** with methyl iodide proceeds quantitatively. In contrast to **2**, the reaction of dianionic NHC **IIb** with methyl iodide solely afforded the methylated derivative and no ethylated product was observed.^[12] The different behavior of **2** and **IIb** may be explained by the higher steric hinderance of **IIb** or the different electronic properties of both NHCs and consequently of the related C2-methylated derivatives. Single crystals of ${}^3_\infty[3\text{-Li}(\text{H}_2\text{O})]$ were obtained from the reaction mixture under air (Figure 5). The Li cation is coordinated to three CN groups of different imidazole units and to one aqua ligand. Thus, the structure exemplifies the coordination ability of the tricyanoborane moiety even in case of neutral imidazole derivatives such as **3**.

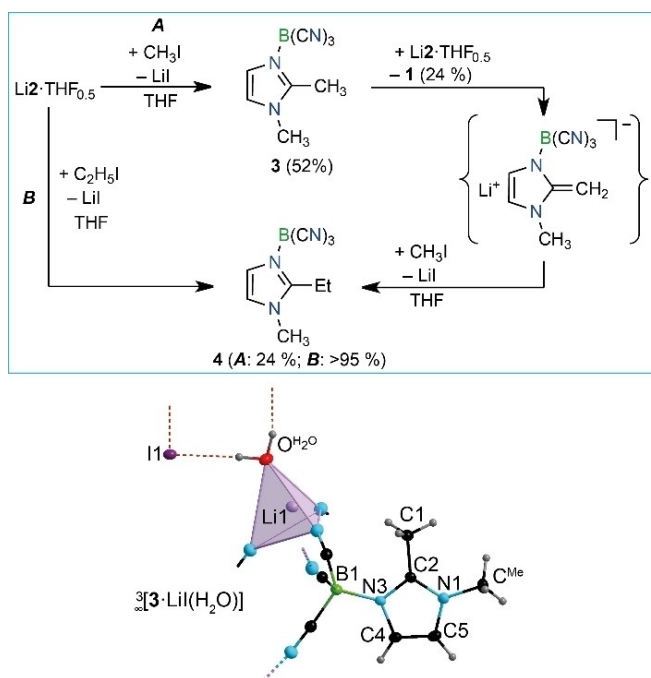


Figure 5. Formation of a mixture of **3**, **4**, and **1** and selective synthesis of **4** by ethylation of **Li2** (top) and crystal structure of ${}^3_\infty[3\text{-Li}(\text{H}_2\text{O})]$ (ellipsoids are drawn at the 50% probability level except for the H atoms that are depicted with arbitrary radii).

The reaction of Li2 with elemental selenium gave the selenourea derivative Li5 in a yield of 96% (Figure 6). In analogy to Li2·THF_{0.5}, Li5·THF_{0.5} contains half an equivalent of THF per formula unit, which was confirmed by NMR spectroscopy and elemental analysis. Crystallization of Li5 from wet THF afforded single crystals of ³_∞[Li5(H₂O)]. The tetrahedral coordination at Li is composed of three cyano groups and an aqua ligand (Figure 6). The C=Se distance with 185.3(5) pm lies in the typical range observed for selenoureas, for instance 185.2(2) in ³_∞[Li2Vb(H₂O)₃]^[12] or 184.2(4) in Va.^[30] ³_∞[Li5(H₂O)] reveals weak Se···H₂O bonds^[31] of 279.1(14) and 281.5(12) (Figure 6), similar to ³_∞[Li2Vb(H₂O)₃] (279(2) and 281(2) pm).^[12]

The ⁷⁷Se chemical shift of Li5 was observed at 74.8 ppm in (CD₃)₂CO, which fits almost perfectly between the shifts of Vb (139.1 ppm)^[12] and Va (8.5 ppm) (Figure 6). δ(⁷⁷Se) is a well-accepted measure for the π-acceptor ability, in general.^[32] So, the increasing δ(⁷⁷Se) with increasing number of B(CN)₃ groups indicates an increasing π-acceptor ability in the row IIa < 2 < IIb, as predicted by theory. The ¹J(⁷⁷Se, ¹³C) coupling constant of 5

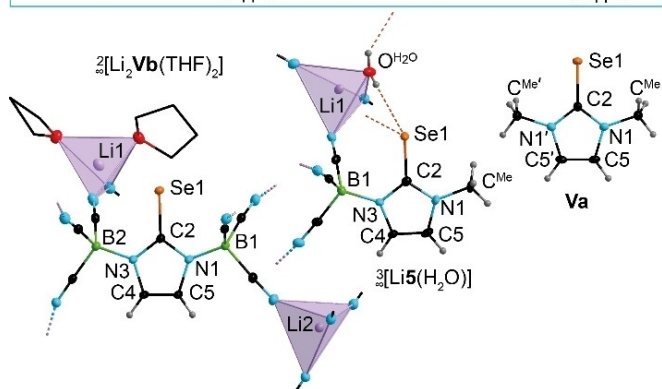
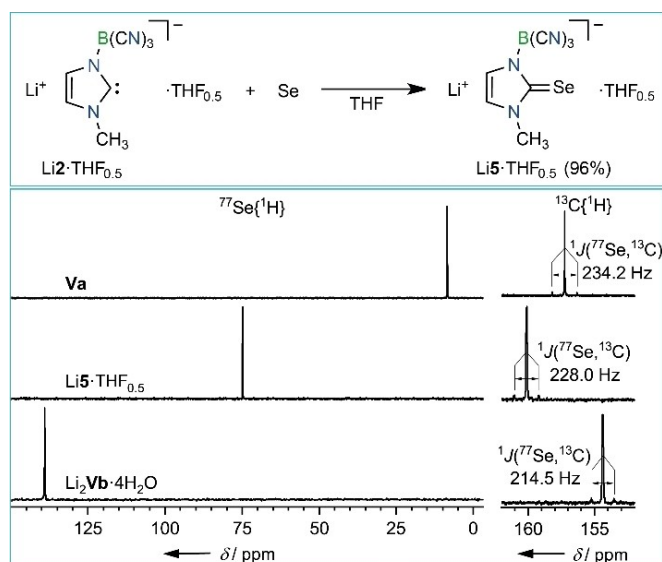


Figure 6. Syntheses of Li5·THF_{0.5} (top), NMR spectra of Va, Li5·THF_{0.5}, and Li₂Vb·4H₂O (middle), and crystal structures of Va,^[30] ³_∞[Li5(H₂O)], and ²_∞[Li₂Vb(THF)₂]^[12] (ellipsoids are drawn at the 50% (³_∞[Li5(H₂O)]) and Va) or 30% (²_∞[Li₂Vb(THF)₂]) probability level except for H atoms that are depicted with arbitrary radii; partial disorder of the imidazolin-2-ylidene ring in ²_∞[Li₂Vb(THF)₂] and disorder and H atoms of the THF solvate molecules are omitted for clarity; the C atoms of THF are shown as stick model in ²_∞[Li₂Vb(THF)₂].

(228.0 Hz) is smaller than the one of Va (234.4 Hz) but larger than the one of Vb (214.5) (Figure 6).^[12] An analogous trend is observed for ¹J(¹³C, ¹H) in DMSO-d₆ for the parent imidazole derivatives that decrease in the order 1,3-dimethylimidazolium cation (Ia, 221.9 Hz, counterion I⁻), 1 (220.3 Hz), and 1,3-bis(tricyanoborane)imidazolate anion (Ib, 217.8 Hz). Both coupling constants ¹J(⁷⁷Se, ¹³C) and ¹J(¹³C, ¹H) are indicative for the σ-donor strength of the corresponding NHC,^[32b,e] which increases with decreasing coupling constants. Thus, the σ-donor strength increases in the same order as the π-acceptor ability (IIa < 2 < IIb). Both experimental trends are in line with those derived from quantum chemical calculations (see above).

In analogy to the syntheses of anionic selenoureas 5 and Vb, the homologous NHC chalcogen derivatives of 2 and IIb using sulfur and tellurium were obtained. The reaction of Li2 with S₈ gave Li6·THF_{0.5}, which was isolated in a yield of 96%. Similarly, Li₂II was reacted with elemental sulfur to yield 71% of Li₂VIIb. Both sulfur compounds are stable against water and air. The crystal structures of ³_∞[Li6(H₂O)] and ³_∞[Li₂VIIb(THF)₂] emphasize the ditopic nature of the B(CN)₃-imidazoline compounds (Figure 7). The C=S distances 169.7(3) pm (³_∞[Li6(H₂O)]) and 167.5 pm (³_∞[Li₂VIIb(THF)₂]) are in the typical range observed for d(C=S) of thioureas, for instance 168.1(5) pm for the corresponding 1,3-dimethyl substituted thiourea VIa.^[33] The tellurium derivatives of Li2 and Li₂II were synthesized, as well. Li7·THF and LiVIIb·(THF)₄ are sensitive towards moisture, air, and light,

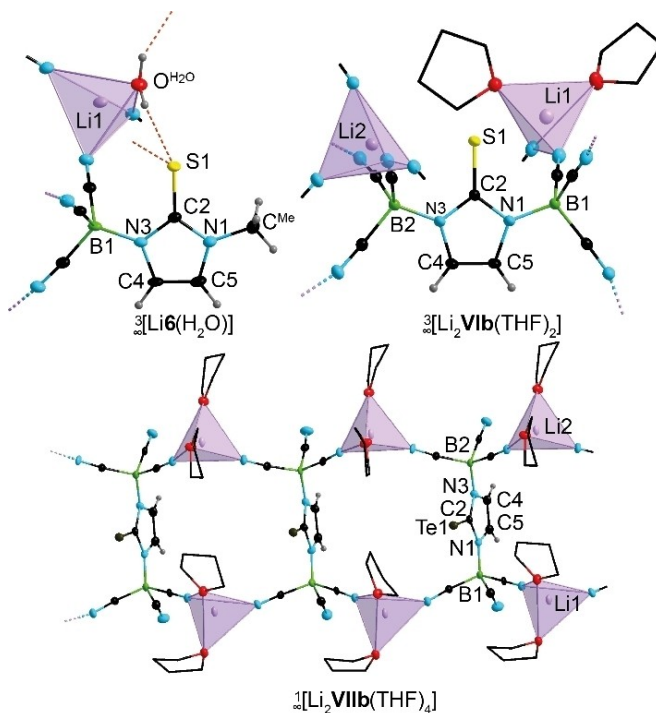


Figure 7. Crystal structures of ³_∞[Li6(H₂O)], ³_∞[Li₂VIIb(THF)₂], and ¹_∞[Li₂VIIb(THF)₄] (ellipsoids are drawn at the 50% (³_∞[Li6(H₂O)]) or 35% (³_∞[Li₂VIIb(THF)₂]) and ¹_∞[Li₂VIIb(THF)₄]) probability level except for the H atoms that are depicted with arbitrary radii; partial disorder of the imidazolin-2-ylidene ring and disorder and H atoms of the THF solvate molecules of ³_∞[Li₂VIIb(THF)₂] are omitted for clarity and the C atoms of the THF molecules are shown as stick model).

which is in agreement to reports on related NHC-tellurium compounds.^[9c] The crystal structure of ${}^1_{\infty}[\text{Li}_2\text{VIIIb}(\text{THF})_4]$ exhibits a chain pattern with bridging lithium cations (Figure 7). The C=Te distance of 207.6(10) pm is similar to $d(\text{C}=\text{Te})$ in related compounds, for example 207.6(2) in $\text{Li}[\{(\text{C}_6\text{F}_5)_3\text{B}\}\text{IDippTe}]$ ^[9c] and 205.5(3) in IDippTe .^[34]

The reaction of nickel tetracarbonyl with Li_2 gave the anionic nickel tricarbonyl complex **8**, which was isolated as lithium salt $\text{Li}^+\cdot\text{THF}$ in 86% yield (Figure 8). For a further assessment of the relative donor strength of the anionic NHC **2**, neutral **IIa**, and dianionic **IIb**, the Tolman electronic parameter (TEP),^[35] which is defined as the $\nu_{\text{CO}}(\text{A}_1)$ band position of $[\text{LNi}(\text{CO})_3]$ with L being a two electron donor ligand, was determined. The IR spectra of $[(\text{IIa})\text{Ni}(\text{CO})_3]$ (**VIIa**),^[36] $\text{Li}^+\cdot\text{THF}$, and $[(\text{IIb})\text{Ni}(\text{CO})_3]^{2-}$ (**VIIIb**)^[12] were measured in THF solution to minimize coordination effects of the lithium counter ions and the respective section of the spectra are depicted in Figure 8. In accordance with the quantum chemical calculations (Figure 4), ${}^1J(^{77}\text{Se},^{13}\text{C})$, and ${}^1J(^{13}\text{C},^1\text{H})$, the TEP of **8** (2048 cm^{-1}) is in-between those of **VIIa** (2050 cm^{-1}) and **VIIIb** (2045 cm^{-1}), which shows that the donor strength of **IIa**, **2**, and **IIb** depends on the number of $\text{B}(\text{CN})_3$ groups attached.

The crystal structure analysis of ${}^3_{\infty}[\text{Li}^+\cdot\text{THF}]$ reveals a tetrahedral coordination at lithium composed of three CN groups and one THF molecule and the common tetrahedral coordination at Ni^0 (Figure 8). The $\text{Ni}^0-\text{C}2$ bond of 197.2(4) pm

is in the range typically observed for NHC nickel tricarbonyl complexes, for example **VIIIb** (198.4(5) pm),^[12] $[(\text{IMes})\text{Ni}(\text{CO})_3]$ (197.1(3) pm), and $[(\text{IDipp})\text{Ni}(\text{CO})_3]$ (197.9(3) pm).^[37] The buried volume ($\%V_{\text{bur}}$)^[38] of the dianionic NHC **2** was estimated to 32.8% from the crystal structure of ${}^3_{\infty}[\text{Li}^+\cdot\text{THF}]$. It is thus smaller than $\%V_{\text{bur}}$ determined for **IIb** (39.9%), which reflects the sterically less demanding methyl group compared to $\text{B}(\text{CN})_3$. The buried volume of **2** is similar to for example IDipp ($\%V_{\text{bur}} = 29\%$).^[37] However, the steric shielding in **2** is highly unsymmetrical, due to the different steric demands of the $\text{B}(\text{CN})_3$ and methyl group (Figure 8).

Conclusion

The tricyanoborane-substituted imidazole **1** and salts of the related anionic NHC **2**, the 1-methyl-3-(tricyanoborane)imidazolin-2-ylidene anion, have been obtained in high yield on gram scale. Anion **2** is a novel unsymmetrical ditopic ligand with promising σ -donor and π -acceptor abilities demonstrated, for example, with the Ni^0 complex ${}^3_{\infty}[\text{Li}^+\cdot\text{THF}]$ (${}^3_{\infty}[\text{Li}^+\cdot\text{THF}]$) and the potassium coordination polymer ${}^3_{\infty}[\text{K}^+\cdot\text{THF}]$. Furthermore, anionic NHC **2** closes the gap between the well-established neutral Arduengo-type carbenes **A**^[1] (Figure 1), for example 1,3-dimethylimidazolin-2-ylidene (IME, **IIa**),^[24] and the recently published dianionic NHC, the bis(tricyanoborane)imidazolin-2-ylidene dianion **IIb**.^[12] According to results of first quantum chemical calculations, NMR spectroscopic data of the selenium adducts of IMe (**IIa**), **2**, and **IIb** (Figure 6) and the TEM of the Ni^0 complexes **VIIa**, **8**, and **VIIIb** (Figure 8), the electronic properties of NHCs can be effectively tuned by the number of $\text{B}(\text{CN})_3$ groups at the NHC core. Both, σ -donor strength and π -acceptor ability increase with increasing number of $\text{B}(\text{CN})_3$ groups. Especially the enhancement of the acceptor ability is surprising and may be rationalized by the participation of the CN groups in the π orbitals (Figure 4). In addition, the introduction of the bulky $\text{B}(\text{CN})_3$ group enables a tuning of the buried volume ($\%V_{\text{bur}}$). This customizability combined with the ease of accessibility renders tricyanoborane-imidazol-2-ylidenates a novel, outstanding class of NHCs.

Experimental Section

Single-crystal X-ray diffraction

Single-crystal X-ray diffraction: Deposition Numbers 2132207 (for **1**), 2132208 (for ${}^2_{\infty}[\text{Li}_2(\text{thf})]$), 2132209 (for $[\{\text{Li}(12\text{-crown-4})\}_2]\cdot(12\text{-crown-4})$), 2132210 (for ${}^3_{\infty}[\text{K}_2(\text{thf})]$), 2132211 (for ${}^3_{\infty}[\text{Li}(\text{H}_2\text{O})]$), 2132212 (for ${}^3_{\infty}[\text{Li}_5(\text{H}_2\text{O})]$), 2132213 (for **Va**), 2132214 (for ${}^3_{\infty}[\text{Li}_6(\text{H}_2\text{O})]$), 2132215 (for ${}^3_{\infty}[\text{Li}_2\text{VIIb}(\text{thf})_2]$), 2132216 (for ${}^3_{\infty}[\text{Li}^+\cdot\text{THF}]$), and 2132217 (for ${}^1_{\infty}[\text{Li}_2\text{VIIIb}(\text{thf})_4]$), contain the supplementary crystallographic data for this paper. These data are provided free of charge by the joint Cambridge Crystallographic Data Centre and Fachinformationszentrum Karlsruhe Access Structures service.

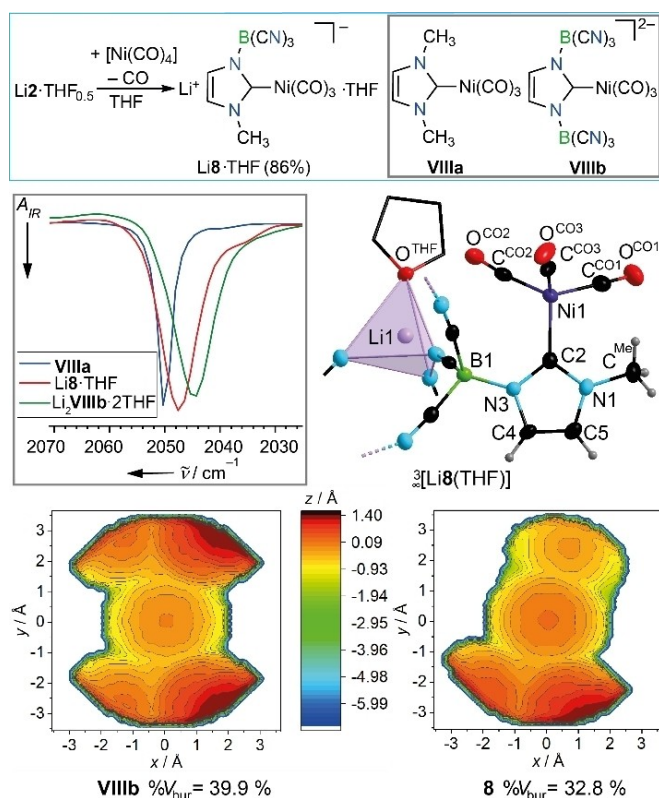


Figure 8. Synthesis of $\text{Li}^+\cdot\text{THF}$ (top), IR spectra of **VIIa**, $\text{Li}^+\cdot\text{THF}$, and $\text{Li}_2\text{VIIIb} \cdot 2\text{THF}$ (middle, left), crystal structure of ${}^3_{\infty}[\text{Li}^+\cdot\text{THF}]$ (ellipsoids are drawn at the 50% probability level except for H atoms that are depicted with arbitrary radii), and steric maps of **VIIIb** and **8**.

Acknowledgements

The authors thank the Julius-Maximilians-Universität Würzburg and the Studienstiftung des Deutschen Volkes (L.Z.) for generous support.

Acknowledgements

Open Access funding enabled and organized by Projekt DEAL.

Conflict of Interest

The authors declare no conflict of interest.

Data Availability Statement

The data that support the findings of this study are available in the supplementary material of this article.

Keywords: N-heterocyclic carbene · anionic carbene · boron · cyanoborate · imidazolate

- [1] a) W. A. Herrmann, C. Köcher, *Angew. Chem. Int. Ed.* **1997**, *36*, 2162–2187; *Angew. Chem.* **1997**, *109*, 2256–2282; b) D. Bourissou, O. Guerret, F. P. Gabbaï, G. Bertrand, *Chem. Rev.* **2000**, *100*, 39–91; c) N-Heterocyclic Carbenes in *Transition Metal Catalysis, Topics in Organometallic Chemistry, Vol. 21*, F. Glorius, Springer-Verlag, Berlin Heidelberg, **2007**; d) F. E. Hahn, M. C. Jahnke, *Angew. Chem. Int. Ed.* **2008**, *47*, 3122–3172; *Angew. Chem.* **2008**, *120*, 3166–3216; e) W. Kirmse, *Angew. Chem. Int. Ed.* **2010**, *49*, 8798–8801; *Angew. Chem.* **2010**, *122*, 8980–8983; f) L. Mercks, M. Albrecht, *Chem. Soc. Rev.* **2010**, *39*, 1903–1912; g) M. Asay, C. Jones, M. Driess, *Chem. Rev.* **2011**, *111*, 354–396; h) L. Benhamou, E. Chardon, G. Lacvigne, S. Bellemin-Laponnaz, V. César, *Chem. Rev.* **2011**, *111*, 2705–2733; i) N-Heterocyclic Carbenes in *Transition Metal Catalysis and Organocatalysis, Catalysis by Metal Complexes, Vol. 32*, C. S. J. Cazin, Springer Science + Business Media B. V., Dordrecht Heidelberg London New York, **2011**; j) C. D. Martin, M. Soleilhavoup, G. Bertrand, *Chem. Sci.* **2013**, *4*, 3020–3030; k) M. N. Hopkinson, C. Richter, M. Schedler, F. Glorius, *Nature (London)* **2014**, *510*, 485–496; l) Y. Wang, G. H. Robinson, *Inorg. Chem.* **2014**, *53*, 11815–11832; m) M. H. Wang, K. A. Scheidt, *Angew. Chem. Int. Ed.* **2016**, *55*, 14912–14922; *Angew. Chem.* **2016**, *128*, 15134–15145; n) S. Würtemberger-Pietsch, U. Radius, T. B. Marder, *Dalton Trans.* **2016**, *45*, 5880–5895; o) E. Peris, *Chem. Rev.* **2018**, *118*, 9988–10031; p) V. V. Nesterov, D. Reiter, P. Bag, P. Frisch, R. Holzner, A. Porzelt, S. Inoue, *Chem. Rev.* **2018**, *118*, 9678–9842; q) S. C. Sau, P. K. Hota, S. K. Mandal, M. Soleilhavoup, G. Bertrand, *Chem. Soc. Rev.* **2020**, *49*, 1233–1252; r) F. Nahra, D. J. Nelson, S. P. Nolan, *Trends Chem.* **2020**, *2*, 1096–1113.
- [2] A. J. Arduengo, R. L. Harlow, M. Kline, *J. Am. Chem. Soc.* **1991**, *113*, 361–363.
- [3] A. Nasr, A. Winkler, M. Tamm, *Coord. Chem. Rev.* **2016**, *316*, 68–124.
- [4] U. Kernbach, M. Ramm, P. Luger, W. P. Fehlhammer, *Angew. Chem. Int. Ed.* **1996**, *35*, 310–312; *Angew. Chem.* **1996**, *108*, 333–335.
- [5] C. Santini, M. Marinelli, M. Pellei, *Eur. J. Inorg. Chem.* **2016**, 2312–2331.
- [6] A. Wacker, H. Pritzkow, W. Siebert, *Eur. J. Inorg. Chem.* **1998**, 843–849.
- [7] a) A. Wacker, H. Pritzkow, W. Siebert, *Eur. J. Inorg. Chem.* **1999**, 789–793; b) A. Wacker, C. G. Yan, G. Kaltenpoth, A. Ginsberg, A. M. Arif, R. D. Ernst, H. Pritzkow, W. Siebert, *J. Organomet. Chem.* **2002**, *641*, 195–202.
- [8] S. Kronig, E. Theuergarten, C. G. Daniliuc, P. G. Jones, M. Tamm, *Angew. Chem. Int. Ed.* **2012**, *51*, 3240–3244; *Angew. Chem.* **2012**, *124*, 3294–3298.
- [9] a) J. Frosch, M. Koneczny, T. Bannenber, M. Tamm, *Chem. Eur. J.* **2021**, *27*, 4349–4363; b) L. P. Ho, L. Anders, M. Tamm, *Chem. Asian J.* **2020**, *15*, 845–851; c) L. P. Ho, L. Körner, T. Bannenber, M. Tamm, *Dalton Trans.* **2020**, *49*, 13207–13217.
- [10] a) E. L. Kolychev, S. Kronig, K. Brandhorst, M. Freytag, P. G. Jones, M. Tamm, *J. Am. Chem. Soc.* **2013**, *135*, 12448–12459; b) K. Nomura, G. Nagai, A. Nasr, K. Tsutsumi, Y. Kawamoto, K. Koide, M. Tamm, *Organometallics* **2019**, *38*, 3233–3244; c) M. Koneczny, L. P. Ho, A. Nasr, M. Freytag, P. G. Jones, M. Tamm, *Adv. Synth. Catal.* **2020**, *362*, 3857–3863.
- [11] D. Vagedes, G. Kehr, D. König, K. Wedeking, R. Fröhlich, G. Erker, C. Mück-Lichtenfeld, S. Grimme, *Eur. J. Inorg. Chem.* **2002**, 2015–2021.
- [12] L. Zapf, U. Radius, M. Finze, *Angew. Chem. Int. Ed.* **2021**, *60*, 17974–17980; *Angew. Chem.* **2021**, *133*, 18118–18125.
- [13] H. Böhler, N. Trapp, D. Himmel, M. Schleep, I. Krossing, *Dalton Trans.* **2015**, *44*, 7489–7499.
- [14] N. V. Ignat'ev, M. Finze, *Eur. J. Inorg. Chem.* **2019**, 3539–3560.
- [15] a) B. Györi, J. Emri, I. Fehér, *J. Organomet. Chem.* **1983**, *255*, 17–28; b) C. Kerpen, J. A. P. Sprenger, L. Herkert, M. Schäfer, L. A. Bischoff, P. Zeides, M. Grüne, R. Bertermann, F. A. Brede, K. Müller-Buschbaum, N. V. Ignat'ev, M. Finze, *Angew. Chem. Int. Ed.* **2017**, *56*, 2800–2804; *Angew. Chem.* **2017**, *129*, 2844–2848; c) L. A. Bischoff, M. Drisch, C. Kerpen, P. T. Hennig, J. Landmann, J. A. P. Sprenger, R. Bertermann, M. Grüne, Q. Yuan, J. Warneke, X.-B. Wang, N. V. Ignat'ev, M. Finze, *Chem. Eur. J.* **2019**, *25*, 3560–3574.
- [16] a) E. Bernhardt, M. Finze, H. Willner, *Z. Anorg. Allg. Chem.* **2003**, *629*, 1229–1234; b) M. Drisch, L. A. Bischoff, J. A. P. Sprenger, P. T. Hennig, R. Wirthensohn, S. Z. Konieczka, M. Hailmann, N. V. Ignat'ev, M. Finze, *Chem. Eur. J.* **2020**, *26*, 11625–11633.
- [17] L. A. Bischoff, J. A. P. Sprenger, P. T. Hennig, N. V. Ignat'ev, M. Finze, *Z. Anorg. Allg. Chem.* **2018**, *644*, 1285–1292.
- [18] a) E. Bernhardt, G. Henkel, H. Willner, *Z. Anorg. Allg. Chem.* **2000**, *626*, 560–568; b) D. J. Williams, B. Pleune, J. Kouvetakis, M. D. Williams, R. A. Andersen, *J. Am. Chem. Soc.* **2000**, *122*, 7735–7741.
- [19] N. Schopper, J. A. P. Sprenger, L. Zapf, G. J. Reiss, N. V. Ignat'ev, M. Finze, *New J. Chem.* **2021**, *45*, 14973–14987.
- [20] J. Landmann, J. A. P. Sprenger, P. T. Hennig, R. Bertermann, M. Grüne, F. Würthner, N. V. Ignat'ev, M. Finze, *Chem. Eur. J.* **2018**, *24*, 608–623.
- [21] a) M. L. Kuhlman, H. Yao, T. B. Rauchfuß, *Chem. Commun.* **2004**, 1370–1371; b) J. Landmann, P. T. Hennig, N. V. Ignat'ev, M. Finze, *Chem. Sci.* **2017**, *8*, 5962–5968.
- [22] a) J. Landmann, J. A. P. Sprenger, M. Hailmann, V. Bernhardt-Pitchougina, H. Willner, N. Ignat'ev, E. Bernhardt, M. Finze, *Angew. Chem. Int. Ed.* **2015**, *54*, 11259–11264; *Angew. Chem.* **2015**, *127*, 11411–11416; b) Y. T. A. Wong, J. Landmann, M. Finze, D. L. Bryce, *J. Am. Chem. Soc.* **2017**, *139*, 8200–8211.
- [23] a) E. Bernhardt, V. Bernhardt-Pitchougina, H. Willner, N. V. Ignatiev, *Angew. Chem. Int. Ed.* **2011**, *50*, 12085–12088; *Angew. Chem.* **2011**, *123*, 12291–12294; b) J. Landmann, J. A. P. Sprenger, R. Bertermann, N. Ignat'ev, V. Bernhardt-Pitchougina, E. Bernhardt, H. Willner, M. Finze, *Chem. Commun.* **2015**, *51*, 4989–4992; c) J. Landmann, F. Keppner, D. B. Hofmann, J. A. P. Sprenger, M. Häring, S. H. Zottnick, K. Müller-Buschbaum, N. V. Ignat'ev, M. Finze, *Angew. Chem. Int. Ed.* **2017**, *56*, 2795–2799; *Angew. Chem.* **2017**, *129*, 2839–2843.
- [24] A. J. Arduengo, H. V. R. Dias, R. L. Harlow, M. Kline, *J. Am. Chem. Soc.* **1992**, *114*, 5530–5534.
- [25] a) A. V. G. Chizmeshya, C. J. Ritter, T. L. Groy, J. B. Tice, J. Kouvetakis, *Chem. Mater.* **2007**, *19*, 5890–5901; b) J. Rießer, L. Zapf, M. Finze, *unpublished results* **2021**.
- [26] A. J. Arduengo, M. Tamm, J. C. Calabrese, F. Davidson, W. J. Marshall, *Chem. Lett.* **1999**, 1021–1022.
- [27] A. Koch, H. Görls, S. Kriech, M. Westerhausen, *Dalton Trans.* **2017**, *46*, 9058–9067.
- [28] a) U. Radius, F. M. Bickelhaupt, *Organometallics* **2008**, *27*, 3410–3414; b) U. Radius, F. M. Bickelhaupt, *Coord. Chem. Rev.* **2009**, *253*, 678–686; c) M. J. Krahfuß, J. Nitsch, F. M. Bickelhaupt, T. B. Marder, U. Radius, *Chem. Eur. J.* **2020**, *26*, 11276–11292.
- [29] a) A. Fürstner, M. Alcarazo, R. Goddard, C. W. Lehmann, *Angew. Chem. Int. Ed.* **2008**, *47*, 3210–3214; *Angew. Chem.* **2008**, *120*, 3254–3258; b) V. B. Saptal, B. M. Bhanage, *ChemSusChem* **2016**, *9*, 1980–1985.
- [30] D. J. Williams, M. R. Fawcett-Brown, R. R. Raye, D. VanDerveer, Y. T. Pang, R. L. Jones, K. L. Bergbauer, *Heteroat. Chem.* **1993**, *4*, 409–414. The crystal structure of **IIa** was determined at 294K; $d(\text{C}=\text{Se}) = 188.4(9)$ pm.
- [31] D. Bibelayi, A. S. Lundemba, F. H. Allen, P. T. A. Galek, J. Pradon, A. M. Reilly, C. R. Groom, Z. G. Yav, *Acta Crystallogr. Sect. B* **2016**, *72*, 317–325.
- [32] a) A. Liske, K. Verlinden, H. Buhl, K. Schaper, C. Ganter, *Organometallics* **2013**, *32*, 5269–5272; b) K. Verlinden, H. Buhl, W. Frank, C. Ganter, *Eur. J. Inorg. Chem.* **2015**, 2416–2425; c) S. V. C. Vummaleti, D. J. Nelson, A.

- Poater, A. Gómez-Suárez, D. B. Cordes, A. M. Z. Slawin, S. P. Nolan, L. Cavallo, *Chem. Sci.* **2015**, *6*, 1895–1904; d) G. P. Junor, J. Lorkowski, C. M. Weinstein, R. Jazzar, C. Pietraszuk, G. Bertrand, *Angew. Chem. Int. Ed.* **2020**, *59*, 22028–22033; *Angew. Chem.* **2020**, *132*, 22212–22217; e) H. V. Huynh, *Chem. Rev.* **2018**, *118*, 9457–9492.
- [33] a) D. W. Tomlin, D. P. Campbell, P. A. Fleitz, *Acta Crystallogr.* **1997**, *C53*, 1153–1154; b) B. L. Benac, E. M. Burgess, A. J. Arduengo, *Org. Synth.* **1986**, *64*, 92–95.
- [34] K. Srinivas, P. Suresh, C. N. Babu, A. Sathyanarayana, G. Prabusankar, *RSC Adv.* **2015**, *5*, 15579–15590.
- [35] C. A. Tolman, *Chem. Rev.* **1977**, *77*, 313–348.
- [36] K. Öfele, W. A. Herrmann, D. Mihalios, M. Elison, E. Herdtweck, W. Scherer, J. Mink, *J. Organomet. Chem.* **1993**, *459*, 177–184.
- [37] R. Dorta, E. D. Stevens, N. M. Scott, C. Costabile, L. Cavallo, C. D. Hoff, S. P. Nolan, *J. Am. Chem. Soc.* **2005**, *127*, 2485–2495.
- [38] a) A. Gómez-Suárez, D. J. Nelson, S. P. Nolan, *Chem. Commun.* **2017**, *53*, 2650–2660; b) H. Clavier, S. P. Nolan, *Chem. Commun.* **2010**, *46*, 841–861.

Manuscript received: January 27, 2022

Accepted manuscript online: May 10, 2022

Version of record online: June 1, 2022